Quality assessment of the commercially available alcohol-based hand sanitizers with femtosecond thermal lens spectroscopy

Subhajit Chakraborty [1,2], **Ashwini Kumar Rawat** [3], **Amit Kumar Mishra** [3], **Debabrata Goswami** [Corresp. 1,3]

[1] Centre for Lasers & Photonics, Indian Institute of Technology Kanpur, Indian Institute of Technology, Kanpur, Kanpur, Uttar Pradesh, India
[2] School of Chemistry, The University of Melbourne, Parkville, Victoria 3010, Australia
[3] Chemistry, Indian Institute of Technology, Kanpur, Kanpur, Uttar Pradesh, India

Corresponding Author: Debabrata Goswami
Email address: dgoswami@iitk.ac.in

Using femtosecond-pulse-induced thermal lens spectroscopy (FTLS), we report a novel method for the quality measurements of Alcohol-Based Hand Sanitizers (ABHS). To sustain its effectiveness, the ABHS must contain the recommended concentration of alcohol content. We diluted the hand sanitizer with water to reduce the quantity of alcohol in the mixture and then performed thermal measurements on it. We performed both dual-beam Z-Scan and time-resolved TL measurements to identify the alcoholic content in the ABHS. The Thermal Lens (TL) signal of the solvent is capable of detecting any relative change in the alcohol content in the mixture. Our technique, therefore, emerges as a sensitive tool for quality testing of alcohol-based hand sanitizers.

Quality Assessments of the Commercially Available Alcohol-based Hand Sanitizers with Femtosecond Thermal Lens Spectroscopy

Subhajit Chakraborty[1,2], Ashwini Kumar Rawat[3], Amit Kumar Mishra[3], and Debabrata Goswami[1,3]

[1] Centre for Lasers & Photonics, Indian Institute of Technology Kanpur, Kanpur-208016, India

[2] School of Chemistry, The University of Melbourne, Parkville, Victoria 3010, Australia

[3] Department of Chemistry, Indian Institute of Technology Kanpur, Kanpur-208016 India

*Corresponding author: dgoswami@iitk.ac.in

Abstract:

Using femtosecond-pulse-induced thermal lens spectroscopy, we report a novel method for the quality measurements of Alcohol-Based Hand Sanitizers (ABHS). To sustain its effectiveness, the ABHS must contain the recommended concentration of alcohol content. We diluted the hand sanitizer with water to reduce the quantity of alcohol in the mixture and then performed thermal measurements on it. We performed both dual-beam Z-Scan and time-resolved TL measurements to identify the alcoholic content in the ABHS. The Thermal Lens (TL) signal of the solvent is capable of detecting any relative change in the alcohol content in the mixture. Our technique, therefore, emerges as a sensitive tool for quality testing of alcohol-based hand sanitizers.

Keywords: Thermal Lens Spectroscopy, Femtosecond Laser, Alcohols, Sanitizers.

Introduction:

Hand sanitizers have become a part of our daily life post-Covid-19 pandemic. There are primarily two types of hand sanitizers, alcohol-free hand sanitizers and alcohol-based hand sanitizers (AHBS). The alcohol-free sanitizer uses chemicals having antiseptic qualities to achieve its antimicrobial effects. Depending on their chemical functional groups, these compounds operate and function in various ways [2,3]. ABHS may include one or more types of alcohol, together with additional excipients and humectants. Without the need for water or drying with towels, ABHS can effectively and rapidly eliminate a broad spectrum of microorganisms [4]. ABHS formulations on the market consist of low-viscosity liquids, gels, foams, dispensers, and wipes [5]. The efficacy of ABHS is reliant on the interaction of multiple parameters, including alcohol type and amount, formulation, other components, manufacturing method, and correct usage technique [6].

The alcohol content of ABHS products ranges from 60 to 95% (v/v). The US Centers for Disease Control and Prevention (CDC) recommends a concentration of 60–95% Ethanol (EtOH) or 2-propanol (IPA) mixed with distilled water for alcohol-based hand sanitizers [5,7]. The World Health Organization (WHO) has advised using alcohol-based hand sanitizers in the absence of water to prevent the spread of the coronavirus since the SARS-CoV-2, CoViD-19 outbreak [8].

Because of this recommendation, there is a lot of demand for ABHS. With this heavy demand for sanitizers, the quality of these hand sanitizers is compromised by reducing the alcoholic quantity in the solution [9]. The effectiveness of an ABHS depends on its alcohol concentration; therefore, quality control is crucial to maintain product integrity and to ensure that consumers are purchasing and using products that have virucidal activity against COVID-19. It is, therefore, critical for developing simple and quick measurement techniques for detecting alcohol in ABHS as well as in determining the alcohol content in commercial ABHS to verify that the user is purchasing an effective product.

A few previous attempts have been made for the requirement of quality control. The hand sanitizers have been examined using a qualitative NMR method to check for impurity chemicals [10]. The gas chromatographic method was utilized in order to measure the amount of alcohol present in both commercially available and homemade ABHS that were liquid and gel-based, respectively [9][11]. The quality of the ABHS was also evaluated using NIR spectral data analysis [12].

However, most of these analytical measurements require rigorous experimental treatment. The NMR method demands an expensive instrumentation capability. Other measurement techniques require external calibration and a sensitivity issue exists for low-level impurities [10]. We, therefore, propose a simple yet powerful approach to examine the alcoholic content in a sanitizer using Thermal Lens (TL) spectroscopic technique [13]. The recent work aims to fulfill the requirement of a simple yet powerful tool for quality measurements of these sanitizers.

Thermal lens spectroscopy is a widely used tool for understanding thermo-optical properties [14–18], Nonlinear optical properties [19,20], trace analysis [21], photochemical reactions [22,23], molecular isomerism [24], distinguishing isotopes [25], etc. This spectroscopic tool has already been used to learn about the structural information of molecules [26,27] and intermolecular interactions [28,29].

Thermal lens spectroscopy is a highly sensitive non-destructive spectroscopic technique that can take advantage of localized photothermal heating in liquids. Photothermal heating creates a temperature gradient and a consequent refractive index gradient. The sample then starts to act like a thermally induced lens. The collimated probe beam encounters a spatially modified refractive index inside the sample, which modulates the wavefront. In a time-resolved thermal lens experiment, we quantify the probe beam's relative change due to the pump beam. The measurement continues until the sample reaches a steady state or a thermal equilibrium [30–32].

Experimental Details

The TL measurements were performed by a mode mismatched pump-probe spectroscopic arrangement. A dual output (1560 nm & 780 nm) Er-doped fiber laser was employed as the light source. The 1560 nm beam was used as the pump beam, whereas the 780 nm line was used as the probe source. The pump beam is focused using a convex lens for photothermal heating, and the probe beam is kept collimated over the entire path. The schematic diagram of the experimental setup is given in figure 1.

Figure 1

For the dual beam z-scan experiment, we placed the sample on a motorized translational stage, and then the stage was moved along the pump beam direction. The transmittance of the probe beam as a function of the sample beam was then recorded in a large-area photodetector. A mechanical shutter is placed on the pump beam arm, which allows the pump beam to be incident for a period of 5 seconds and then blocks its incidence for the next 5 seconds. Now for the time-resolved TL measurements, the sample is positioned at the focus of the pump beam, and then we record the transient behavior of the transmitted probe beam.

Mathematical Background and Theoretical Foundations of Thermal Lens Models

The TL signal for dual beam Z-Scan is written in the form of

(1)

$$S(z,t_\infty) = \frac{T(z,t_\infty) - T_0}{T_0}$$

Here $T(z,t_\infty)$ is the transmittance of the probe beam through the aperture in the presence of the pump beam. T_0 is also the same probe beam transmittance but when the pump beam is absent [24]. We recently demonstrated that the most widely used model proposed by Shen et al. is incapable of explaining the unusual thermal lens signatures of alcohols with strong absorption at the pump wavelength, causing a greater heat load inside the sample [13,15]. Later, a new model was developed to account for the thermal lens behavior of highly absorbing samples by incorporating both conductive and convective heat transfer modes[33].

The time-resolved TL signal is defined as follows [34]

$$S(t) = \frac{I(t)}{I(0)} \qquad (2)$$

Where, $I(t)$is the intensity of the probe beam transmitted through an aperture when the pump beam is turned on, whereas $I(0)$ is the intensity of the probe beam transmitted through the aperture when the pump beam is turned off. Now, we can express the steady-state thermal lens signal as

$$S(\infty) = \frac{I(\infty) - I(0)}{I(0)} \qquad (3)$$

Here $I(\infty)$ is considered to be the TL signal after a sufficiently long period of time has passed with no change in the TL signal. The TL signal is additionally written as:

$$TL\,(t) = 1 - S(t) \qquad (4)$$

The following Modified Shen model equation describes the time-resolved thermal lens.

$$\frac{I(t)}{I(0)} = \left[1 - \frac{\theta_1+\theta_2}{2} tan^{-1}\left\{\frac{2mv}{((1+2m)^2+v^2)\frac{t_c}{2t}+1+2m+v^2}\right\}\right]^2 + F\left[\frac{\theta_1+\theta_2}{4}\ln\left(\frac{[1+2m/(1+2t/t_c)]^2+v^2}{(1+2m)^2+v^2}\right)\right]^2 \quad (5)$$

The quantities θ_1,θ_2 and t_c contain all of the sample's properties that affect the strength of the thermal lens. The geometrical parameters are denoted by m and v. which is defined as, $m = {\omega_p}^2/{\omega_e}^2$ and $v = \frac{z_1}{z_c} + \frac{z_c}{z_2}\left[1 + \left(\frac{z_1}{z_c}\right)^2\right]$.

$\theta_1 = -Al\left({dn}/{dT}\right)/\lambda_p\kappa,$ and $\theta_2 = \left[(\alpha(P-A)l\left({dn}/{dT}\right)/\lambda_p h\right]\exp\left(-t_d/t\right) = \theta_{conv}\exp\left(-t_d/t\right),$

${dn}/{dt}$ is the thermo-optic coefficient of the sample, The wavelength of the probe beam is denoted by λ_p, the sample path length is denoted by l, and the absorption coefficient is denoted by A. ω_e denotes the radius of the pump beam, and ω_p denotes the radius of the probe beam at the sample position; P_e denotes the power of the pump beam; $t_c = {\omega_e}^2/4D$, denotes the characteristic time constant, and D denotes the thermal diffusivity.

Sample Preparation

In our experiment, we used three alcohol-based Sanitizers (S1, S2, and S3), which were further diluted with deionized water before the experiments. S1 is an IPA-based sanitizer where the main constituent of S2 is ethyl alcohol (EtOH). The sanitizer S3 is a mix of both IPA & EtOH. These three sanitizers and the other two pure solvents (EtOH & IPA) were mixed with DI water at desired volumetric proportions. These samples were further sonicated at room temperature for 15 minutes.

Results and Discussions

The UV-Vis-NIR absorption spectroscopy of the samples used (Figure 2) gives us an idea of the absorption coefficient of the samples at the pump wavelength. The optical absorption of the pump wavelength is very critical to TL measurements as it is directly correlated to the photothermal heating inside the samples.

Figure 2

Initially, we took three sanitizers in their pure state and then added DI water in order to dilute the alcohol quantity in the newly prepared mixture. After dilution, the volumetric ratio of the sanitizer and water in the immediate next mixture was set to 90:10. Further, we added water to set the ratio o 80:20. So, again, the amount of water in the mixture was increased in intermediate steps of 10%. All three sanitizers and also EtOH & IPA exhibit significant absorption at 1560 nm (Pump Wavelength) [35]. Among these, water has the highest absorption value, and with the increasing quantity of water in the mixtures, the absorption at the pump wavelength enhances. This results in an increment of thermal heat loading in the system during the TL measurements.

Figure 3

Figure 3 (a) depicts the dual beam Z-Scan traces for the pure solvents (viz. EtOH, IPA & water). Among these solvents, IPA & EtOH exhibits a very strong TL signature; however, water has a very low TL signal because of its high thermal conductivity [36,37]. In the case of EtOH & IPA, when the sample is moved towards the focal plane, the thermal load inside the system increases accordingly, resulting in an enhanced lensing effect. Thus, the TL signal is found to increase as the sample moves closer to the focal region. Near the focal area, the beam diameter of the pump beam is minimal, so the intensity of the pump beam is the highest, and so is the heat load. Consequent to the immense heat load, the convective mode of heat transfer comes into the picture as a part of the heat dissipation process. Due to such convective processes, we observe a slow rise

in the TL signal near the focal region. The TL signal exhibits a "W" type signature because of the convective heat transfer mechanisms. Figure 3 (b) represents the dual beam Z-Scan traces of the three sanitizers. Since the main constituent of these sanitizers is either IPA or EtOH, they all are highly sensitive to TL effects and exhibit a very strong TL signal. We can also observe the "W" type TL signature for the sanitizer S2, which is obvious as the main constituent of S2 is EtOH.
Time-resolved TL measurements for the pure solvents are shown in figure 3(c). EtOH & IPA exhibit a strong TL signal in the presence of the pump beam. The TL signal for these two solvents reaches a steady state after passing through the inflection point. The rise of the TL signal from the inflection point to the steady state results from the convective heat transfer processes arising in the system. Water has a comparatively weaker TL response than the other two, which could be attributed to its exalted thermal conductivity. Figure 3(d) represents the time-resolved TL signal for all three investigated sanitizers. As the main constituents of these sanitizers respond positively to the thermal tensing effects, the sanitizers are also highly sensitive to TL effects and exhibit a very strong TL signal during time-resolved measurements.

Figure 4

Figure 4(a), (b), and (c) represent the dual beam Z-Scan traces of the sanitizer S1, S2, and S3, respectively. In all three figures, we observe that the pure sanitizers and their diluted mixtures are very sensitive to the TL measurements. The maximum TL response is observed near the focal plane during the dual beam Z-scan. The amplitude of the TL signal for the pure solvents is found to be the maximum for all three cases. The subsequent addition of water to the mixture reduces the volume fraction of the sanitizer component. From the UV-Vis NIR absorption spectrum (figure 1), we notice that the absorbance value of the mixture at the pump wavelength is increased with the increasing concentration of water in the mixture. As the absorption increases, we expect the thermal heat load deposited to the system also to increase similarly. The enhanced heat load should contribute to a greater TL signal amplitude, but on the contrary, we observe that the TL signal decreases with increasing water concentration.

All these results could be attributed to the very high thermal conductivity of water. Water systems have a very strong hydrogen-bonded network. Consequently, the deposited heat could be transported very effectively in the system, and hence the TL signal decreases although the heat load increases in the system. The highly conductive hydrogen-bonded network of the water molecules takes care of the transportation of the accumulated energy.

Earlier in figure 3, we observed that the main constituents of the sanitizers, i.e., IPA & EtOH, exhibit a convective property, and so do we observe for the pure sanitizers. In figure 4, also we notice a W-type signature in the z-scan traces of the samples for pure sanitizers. However, this feature diminishes upon mixing water in the system. This indicates that the convective effects slowly die out, and conduction is established as a dominating mode of heat transport in the system. When the sanitizer concentration falls below 60% (v/v), the TL signal amplitude is found to fall very sharply, and the TL response of the system is diminished to much extent when the water content is significantly high in the mixture.

Figure 5

Figure 5(a), (b), and (c) represent the time-resolved TL signal of the sanitizers and their diluted mixtures with water. Pure sanitizers exhibit the maximum steady-state TL signal. The steady-state TL signal is found to be decreasing when water is added to the system. Very similar to the dual beam z scan traces, the sharp fall in the steady state TL signal is observed when the sanitizer concentration in the system falls below 60% (v/v). The TL response is also negligible in the time-resolved measurements at very low sanitizer concentrations.

Till now, we have understood the TL signatures of pure sanitizers and their main constituents. We also explored the TL response of the sanitizers when they were diluted with water. However, to understand the TL response in more detail, it is necessary to comprehend the dilution effects on the main constituents of the sanitizers. We further prepared mixtures by diluting EtOH and IPA with water and performed TL measurements with these samples.

Figure 6

Figure 6(a) depicts the dual beam z-scan traces for the IPA-water mixtures. We observe a "w" type feature in the z-scan trace of pure IPA, similar to figure 3, which indicates the presence of convective characteristics in the system. Surprisingly the pure IPA does not exhibit the maximum TL signal amplitude. When water is added to the mixture, we observe the TL signal amplitude increases up to some extent and then decrease upon further addition of water. The convective feature also slowly diminishes when water is added to the system establishing the conductive mode into a dominating mode of heat transfer when the water proportions are significantly large in the system.

Figure 6(b) represents the z-scan traces for EtOH-water mixtures. EtOH also exhibits a very strong convective heat transfer feature in its TL signature. However, these convective effects are diluted upon adding water to the system, similar to the earlier ones. Also, in the TL response of the EtOH-Water mixture, the amplitude of the TL signal is not maximum for the pure EtOH solvent. We observe an initial rise in the TL amplitude when water is mixed into the system. Further addition of water in the mixture leads to a decrement in the TL signal.

The time-resolved TL signatures of the IPA-water mixture are presented in figure 6(c). The inflection points in the TL signatures are evidence of the presence of convective mode. When water is added to pure IPA for dilution purposes, we observe that the steady state TL signal of the mixture increases a little compared to the pure IPA. Further addition of water in the mixture eventually leads to a decrement in the steady state TL signal of the mixture. The inflection point and the convective features slowly vanish with increasing water proportions in the mixture, which could be attributed to the very high thermal conductivity of the water molecules.

Figure 6(d) represents the time-resolved TL signal for EtOH-Water mixtures. The TL response here is also very similar to the earlier one. The steady-state TL signal initially increases on water inclusion and decreases further when the water content exceeds the alcohol content in the mixture. The convective mode of heat transfer is very much present in the mixtures where the alcohol concentration is sufficiently large. Still, these convective characteristics are diminished at concentrations where water molecules are dominating.

An interesting feature in both systems is observed that the pure solvents do not exhibit the highest steady-state TL signal. Rather than the EtOH/IPA (90%)-Water (10%) mixture have a greater TL signal than their pure state. These phenomena arise due to the formation of complex clusters by alcohol and water molecules in the mixtures [38,39]. These clusters are larger, have a very complex shape, and are heavier in size than the standalone alcohol molecules. Therefore, the movement and drifting of these structures are very much restricted compared to the small alcohol molecules. As a result, these molecular complexes have minimal contribution to the convective mode of heat transfer, and the accumulated heat is not carried away smoothly as earlier. Hence, we observe a rise in the steady state TL signal at the initial stages of dilution of alcohols with water.

Figure 7

Figure 7 represents the variation of the steady-state TL signal of the pure solvents and also their diluted mixtures with water. In figure 7(a), we notice the steady-state TL signal decrement when the volume fraction of water increases. Any amount of water added to the sanitizers changes the photothermal response of the mixture, which is reflected in their TL signature. The decrement of the TL signal is very rapid after a substantial amount of water molecules are present in the system. Our TL measurements are sensitive enough to capture any change in the constituents of the mixture. Hence when we dilute the sanitizers with water, the TL measurement is able to reveal the change in its components through a decrement of the steady state TL signal.

Figure 7(b) represents the variation of steady-state TL signals of IPA-water and EtOH-Water mixtures at different volumetric proportions of water. For IPA water mixtures, we observe that the steady state TL signal decreases significantly only after the number of water molecules is near the same or larger than the alcohol molecules. The photothermal response of the mixtures is almost like the pure states when the water molecules are in limited numbers in the mixture. We observe a rapid decrease in the steady state TL signal after IPA (50%) – Water (50%).

For EtOH-water mixtures, we observe that the steady state TL signal increases initially upon the addition of water in the mixture, but later, the TL signal is found to be decreasing with increasing water concentration. Pure EtOH doesn't exhibit the highest TL signal due to its convective features. The initial increase of the TL signal is explained earlier, which is attributed to the formation of complex molecular structures.

However, when we compare the dilution effects in sanitizers and in pure solvents, we find that the TL response of the sanitizer mixture is very prompt compared to the other one. In the case of the sanitizers, we do not observe any initial increment of the TL signal. The intermolecular interaction of the main constituent of sanitizer and water is reduced due to the presence of other impurities, like fragrances, glycerin, colorant, etc., in the local environment. Hence the TL response of the sanitizers is different from that of the pure solvents. Consequently, we can identify the change in the composition of the sanitizer mixtures through our TL measurements.

Conclusions

We performed dual beam Z scan and time-resolved TL measurements of alcohol-based hand sanitizers and their main constituent components IPA & EtOH. We have also conducted TL measurements after diluting the sanitizers with water. The photothermal response was also measured for EtOH and IPA and their mixtures with water to gain greater insight into their intermolecular interactions and dilution effects on heat transfer mechanisms. Our TL measurements appear capable of quantifying the available proportions of alcohols in the sanitizer-water mixtures. Our study correlates the effect of ingredients ratio on the performance of the hand sanitizer. TL measurements could identify any change in the sanitizer compositions; hence, our technique emerges as a sensitive probe to study such complex systems.

Acknowledgment

We acknowledge the funding support of this research from MEITY, SERB, and STC ISRO of the Govt. of India. We thank members of FemtoLab for their support during the experiment. All the authors thank Mrs. S. Goswami for language correction and editing. SC and AKR acknowledge IIT Kanpur for the graduate fellowship. AKM acknowledges IIT Kanpur for Institute PDF support.

Conflict of interest

The authors declare no conflict of interest.

References

[1] Jing J L J, Pei Yi T, Bose R J C, McCarthy J R, Tharmalingam N and Madheswaran T 2020 Hand sanitizers:

a review on formulation aspects, adverse effects, and regulations *Int. J. Environ. Res. Public Health* **17** 3326

[2] Bloomfield S F and Arthur M 1994 Mechanisms of inactivation and resistance of spores to chemical biocides *J. Appl. Bacteriol.* **76** 91S-104S

[3] McDonnell G and Russell A D 1999 Antiseptics and Disinfectants: Activity, Action, and Resistance *Clin. Microbiol. Rev.* **12** 147–79

[4] Lee J, Jing J, Yi T P, Bose R J C, Mccarthy J R, Tharmalingam N and Madheswaran T 2020 Hand Sanitizers: a Review on Formulation Aspects, Adverse Effects, and Regulations *Int. J. Environ. Res. Public Health* **17** 3326

[5] Matatiele P, Southon B, Dabula B, Marageni T, Poongavanum P and Kgarebe B 2022 Assessment of quality of alcohol-based hand sanitizers used in Johannesburg area during the CoViD-19 pandemic *Sci. Rep.* **12** 1–7

[6] Abuga K and Nyamweya N 2021 Alcohol-based hand sanitizers in COVID-19 prevention: a multidimensional perspective *Pharmacy* **9** 64

[7] Boyce J M 2002 CDC guideline for hand hygiene in health-care setting *MMWR* **51** 1–44

[8] Organization W H and others 2020 *Recommendations to Member States to improve hand hygiene practices to help prevent the transmission of the COVID-19 virus: interim guidance, 1 April 2020*

[9] Yusuf A A 2021 Determination of alcohols in hand sanitisers: Are off-the-shelf hand sanitisers what they claim to be? *S. Afr. J. Sci.* **117** 1–7

[10] Bedner M, Murray J, Urbas A A, MacCrehan W A, Wilson W B and others 2021 A Comparison of Measurement Methods for Alcohol-Based Hand Sanitizers *Natl. Inst. Stand. Technol.*

[11] Abuga K, Nyamweya N and King'ondu O 2021 Quality of Alcohol Based Hand Sanitizers Marketed in the Nairobi Metropolitan Area *East Cent. African J. Pharm. Sci.* **24** 29–37

[12] Pasquini C, Hespanhol M C, Cruz K A M L and Pereira A F 2020 Monitoring the quality of ethanol-based hand sanitizers by low-cost near-infrared spectroscopy *Microchem. J.* **159** 105421

[13] Shen J, Lowe R D and Snook R D 1992 A model for cw laser induced mode-mismatched dual-beam thermal lens spectrometry *Chem. Phys.* **165** 385–96

[14] Chakraborty S, Mishra A K, Rawat A K and Goswami D 2021 Understanding the Photothermal Response of CBNP Nanofluids Using Thermal Lens Spectroscopic Techniques *Laser Science* pp JTu1A--99

[15] Singhal S and Goswami D 2020 Unraveling the molecular dependence of femtosecond laser-induced thermal

lens spectroscopy in fluids *Analyst* **145** 929–38

[16] Jiménez-Pérez J L, López Gamboa G, Gutiérrez Fuentes R, Sánchez Ramírez J F, Correa Pacheco Z N, López-y-López V E and Tepech-Carrillo L 2016 Synthesis and thermal properties of new bionanofluids containing gold nanoparticles *Appl. Phys. A Mater. Sci. Process.* **122** 1–6

[17] Jiménez-Pérez J L, Pincel P V, Cruz-Orea A and Correa-Pacheco Z N 2016 Thermal characterization of a liquid resin for 3D printing using photothermal techniques *Appl. Phys. A Mater. Sci. Process.* **122** 556

[18] Oliveira G M, Zanuto V S, Flizikowski G A S, Kimura N M, Sampaio A R, Novatski A, Baesso M L, Malacarne L C and Astrath N G C 2020 Soret effect in lyotropic liquid crystal in the isotropic phase revealed by time-resolved thermal lens *J. Mol. Liq.* **312**

[19] Ventura M, Silva J R, Catunda T, Andrade L H C and Lima S M 2021 Identification of overtone and combination bands of organic solvents by thermal lens spectroscopy with tunable Ti:sapphire laser excitation *J. Mol. Liq.* **328** 115414

[20] Rodriguez L and Chiesa M 2011 Measurement of the two-photon absorption cross section by means of femtosecond thermal lensing *Appl. Opt.* **50** 3240–5

[21] Shokoufi N and Hamdamali A 2010 Laser induced-thermal lens spectrometry in combination with dispersive liquid--liquid microextraction for trace analysis *Anal. Chim. Acta* **681** 56–62

[22] Herculano L S, Astrath N G C, Malacarne L C, Rohling J H, Tanimoto S T and Baesso M L 2011 Laser-induced chemical reaction characterization in photosensitive aqueous solutions *J. Phys. Chem. B* **115** 9417–20

[23] Astrath N G C, Astrath F B G, Shen J, Zhou J, Michaelian K H, Fairbridge C, Malacarne L C, Pedreira P R B, Medina A N and Baesso M L 2009 Thermal-lens study of photochemical reaction kinetics *Opt. Lett.* **34** 3460–2

[24] Kumar P, Dinda S and Goswami D 2014 Effect of molecular structural isomers in thermal lens spectroscopy *Chem. Phys. Lett.* **601** 163–7

[25] Bhattacharyya I, Kumar P and Goswami D 2014 Effect of isotope substitution in binary liquids with Thermal-Lens spectroscopy *Chem. Phys. Lett.* **598** 35–8

[26] Mikheev I V., Usoltseva L O, Ivshukov D A, Volkov D S, Korobov M V. and Proskurnin M A 2016 Approach to the assessment of size-dependent thermal properties of disperse solutions: Time-resolved photothermal

lensing of aqueous pristine fullerenes C60 and C70 *J. Phys. Chem. C* **120** 28270–87

[27] Kumar P and Goswami D 2014 Importance of molecular structure on the thermophoresis of binary mixtures *J. Phys. Chem. B* **118** 14852–9

[28] Chakraborty S, Rawat A K and Goswami D 2019 Sensing the Molecular Properties in Methanol and its Binary Mixtures using Time-Resolved Thermal Lens Spectrometer *2019 Workshop on Recent Advances in Photonics, WRAP 2019*

[29] Bhattacharyya I, Kumar P and Goswami D 2011 Probing intermolecular interaction through thermal-lens spectroscopy *J. Phys. Chem. B* **115** 262–8

[30] Gordon J P, Leite R C C, Moore R S, Porto S P S and Whinnery J R 1965 Long-transient effects in lasers with inserted liquid samples *J. Appl. Phys.*

[31] Hempelmann U and Dorfmueller T 1991 Thermal lens spectroscopy of the phenothiazine dye thionine in solution *J. Mol. Liq.*

[32] John J, Mathew R M, Rejeena I, Jayakrishnan R, Mathew S, Thomas V and Mujeeb A 2019 Nonlinear optical limiting and dual beam mode matched thermal lensing of nano fluids containing green synthesized copper nanoparticles *J. Mol. Liq.*

[33] Kumar P, Khan A and Goswami D 2014 Importance of molecular heat convection in time resolved thermal lens study of highly absorbing samples *Chem. Phys.* **441** 5–10

[34] Singhal S and Goswami D 2019 Thermal Lens Study of NIR Femtosecond Laser-Induced Convection in Alcohols *ACS Omega* **4** 1889–96

[35] Kumar Rawat A, Chakraborty S, Kumar Mishra A and Goswami D 2022 Achieving molecular distinction in alcohols with femtosecond thermal lens spectroscopy *Chem. Phys.* **561** 111596

[36] Simpson S, Schelfhout A, Golden C and Vafaei S 2018 Nanofluid thermal conductivity and effective parameters *Appl. Sci.* **9**

[37] Korson L, Drost-Hansen W and Millero F J 1969 Viscosity of water at various temperatures *J. Phys. Chem.* **73** 34–9

[38] Wakisaka A, Abdoul-Carime H, Yamamoto Y and Kiyozumi Y 1998 Non-ideality of binary mixtures: Water-methanol and water-acetonitrile from the viewpoint of clustering structure *J. Chem. Soc. - Faraday Trans.*

[39] Buhvestov U, Rived F, Ràfols C, Bosch E and Rosés M 1998 Solute-solvent and solvent-solvent interactions

in binary solvent mixtures. Part 7. Comparison of the enhancement of the water structure in alcohol-water mixtures measured by solvatochromic indicators *J. Phys. Org. Chem.*

Figure 1

Schematic diagram of the experimental setup

Schematic Experimental Diagram.

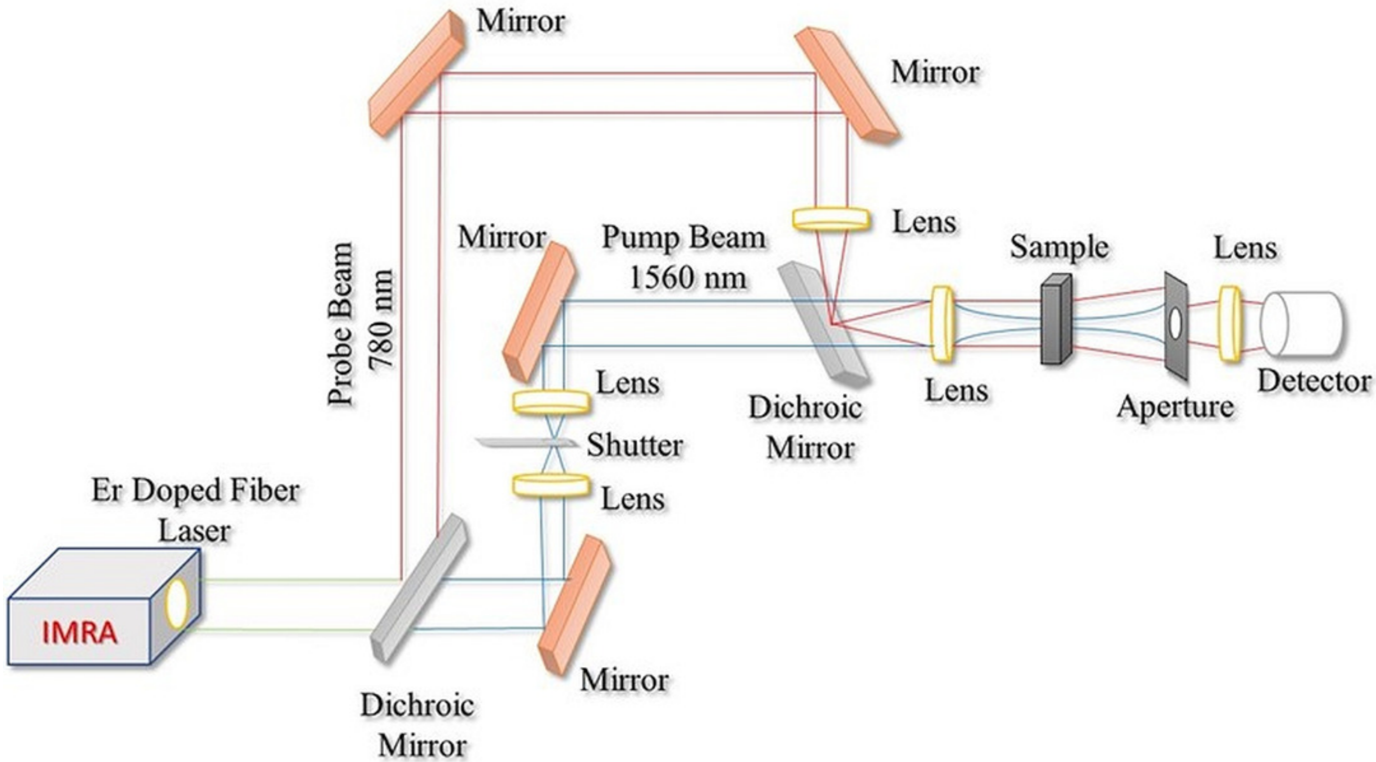

Figure 2

UV-Vis -NIR absorption Spectrum of all the samples used (a), (b), (c), (d) and (e).

The addition of Water in pure solvent increases the absorption of the mixture at 1560 nm for all the samples.

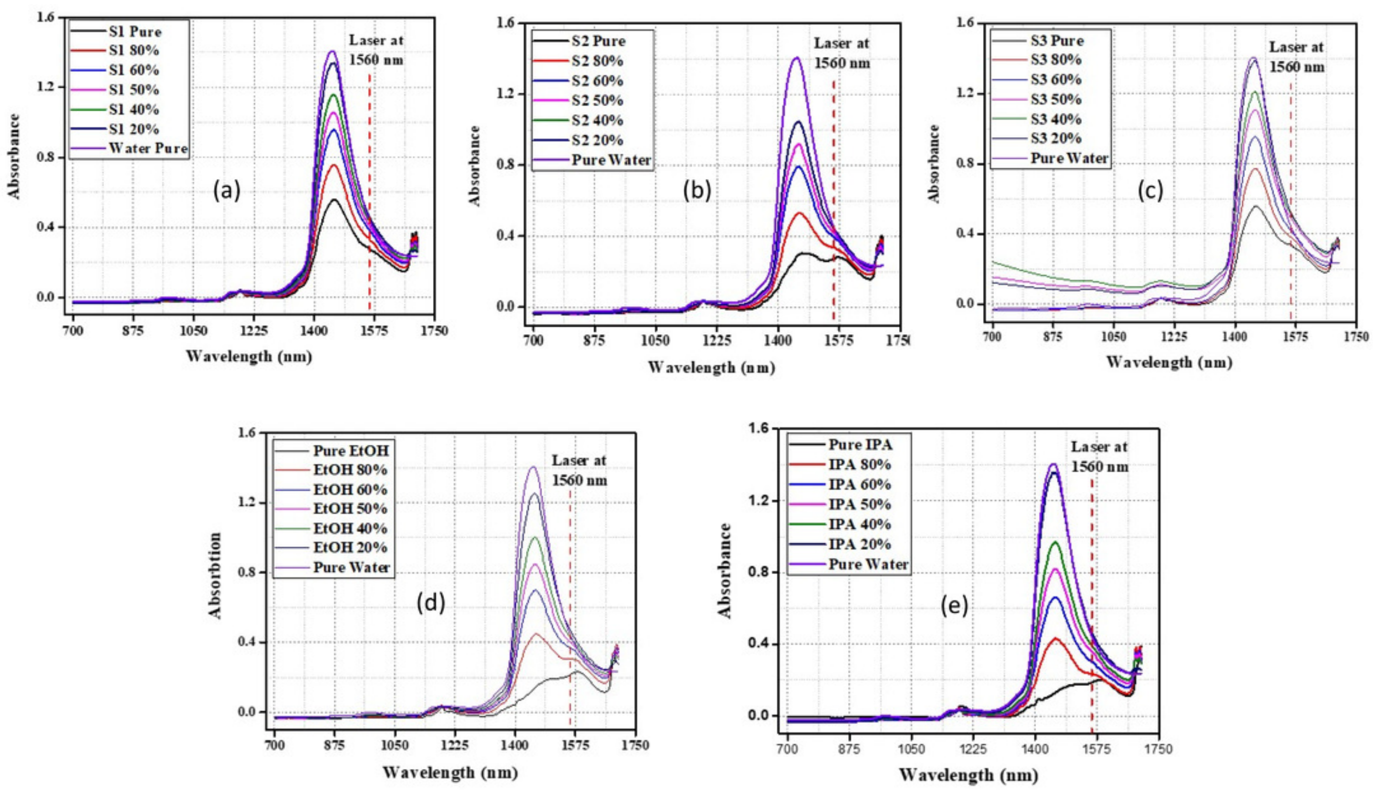

Figure 3

Thermal Lens Spectra of pure solvents

(a) and (b) Dual-beam Z-Scan Thermal Lens Spectra of pure solvents. (c) and (d) Dual-beam Time-resolved TL measurements of Pure solvents.

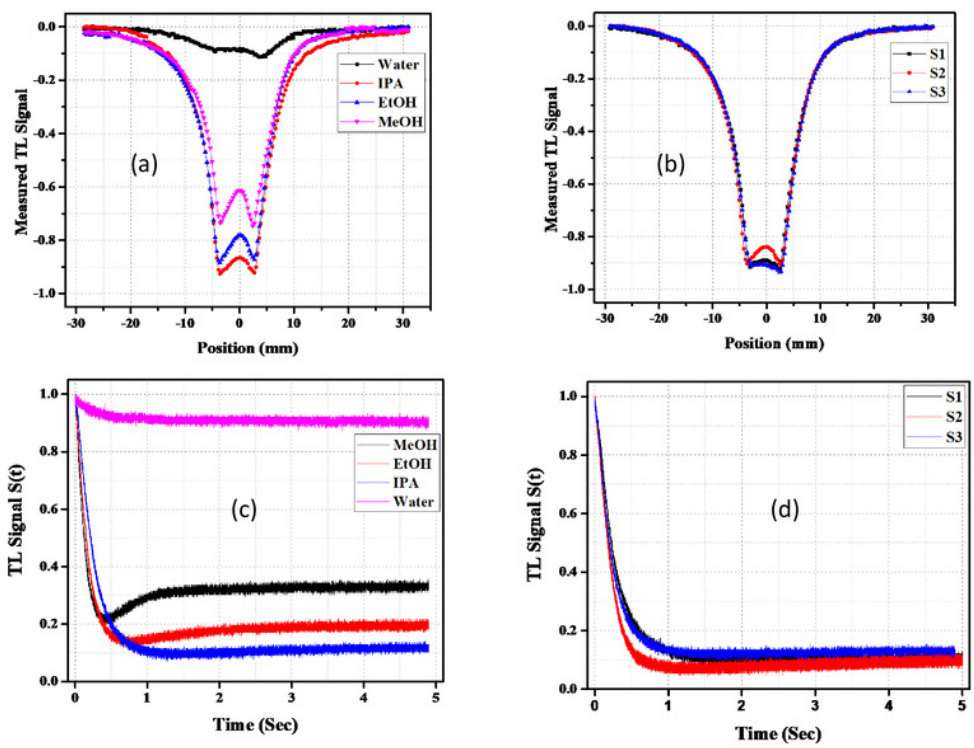

Figure 4

Dual-beam Z-Scan and Time-resolved TL measurements of three sanitizers.

Dual-beam Z-Scan and Time-resolved TL measurements of three sanitizers (S1, S2, and S3) and their mixtures with water.

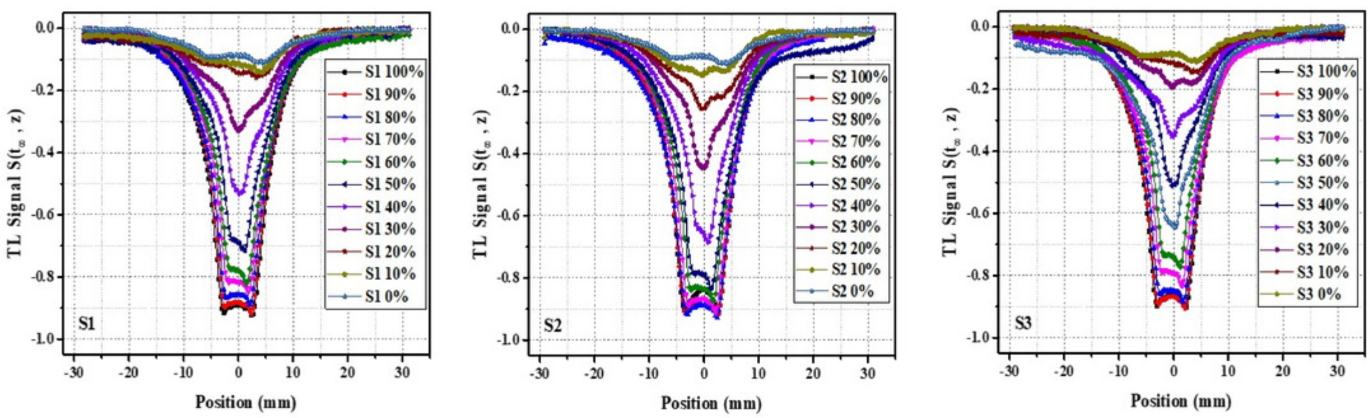

Figure 5

Time-resolved TL signal of the three sanitizers studied.

Time-resolved TL signal of sanitizers (S1, S2, and S3) and their mixtures with water as shown in (a), (b), and (c) respectively.

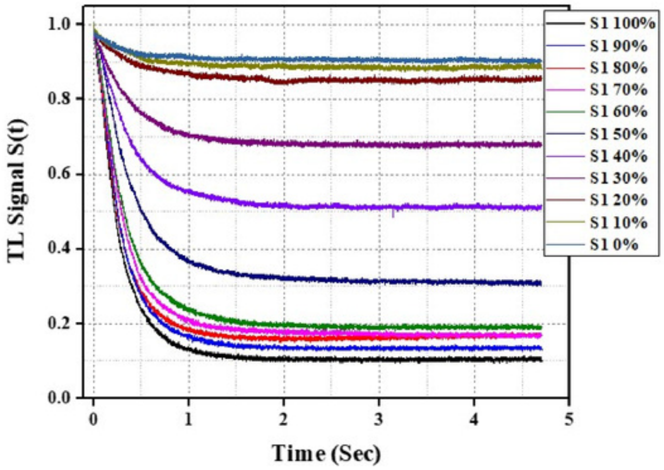
TL Signal S(t)
Time (Sec)
S1 100%
S1 90%
S1 80%
S1 70%
S1 60%
S1 50%
S1 40%
S1 30%
S1 20%
S1 10%
S1 0%

(a)

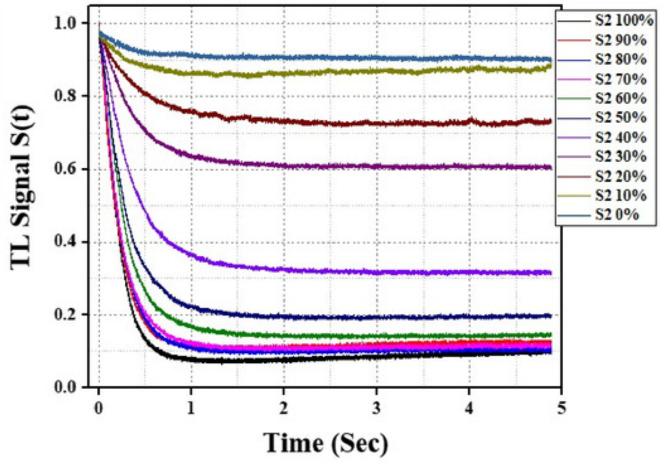
TL Signal S(t)
Time (Sec)
S2 100%
S2 90%
S2 80%
S2 70%
S2 60%
S2 50%
S2 40%
S2 30%
S2 20%
S2 10%
S2 0%

(b)

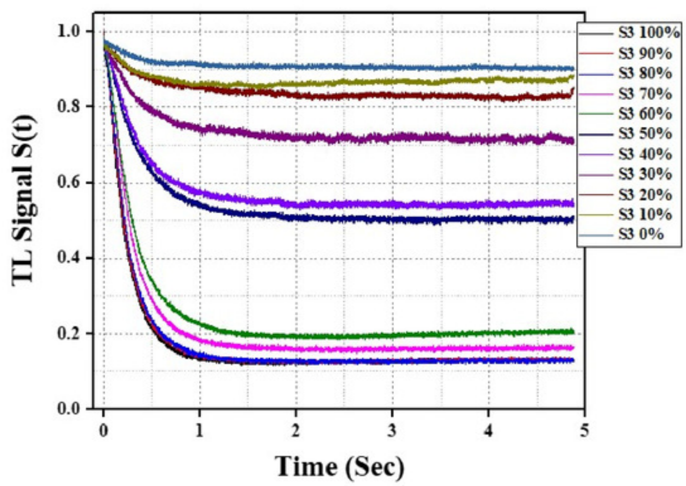
TL Signal S(t)
Time (Sec)
S3 100%
S3 90%
S3 80%
S3 70%
S3 60%
S3 50%
S3 40%
S3 30%
S3 20%
S3 10%
S3 0%

(c)

Figure 6

Dual-beam Z-Scan and Time-resolved TL measurements of sanitizers in mixed solutions

Dual-beam Z Scan traces of (a) IPA-water mixtures, (b) EtOH-Water mixtures, Time-resolved TL signal of (c) IPA-water mixtures, (d) EtOH-Water mixtures

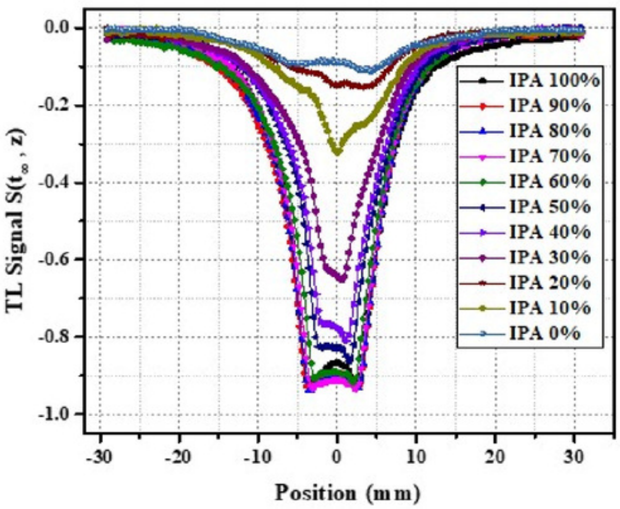
TL Signal S(t∞ , z)
Position (mm)
IPA 100%
IPA 90%
IPA 80%
IPA 70%
IPA 60%
IPA 50%
IPA 40%
IPA 30%
IPA 20%
IPA 10%
IPA 0%

(a)

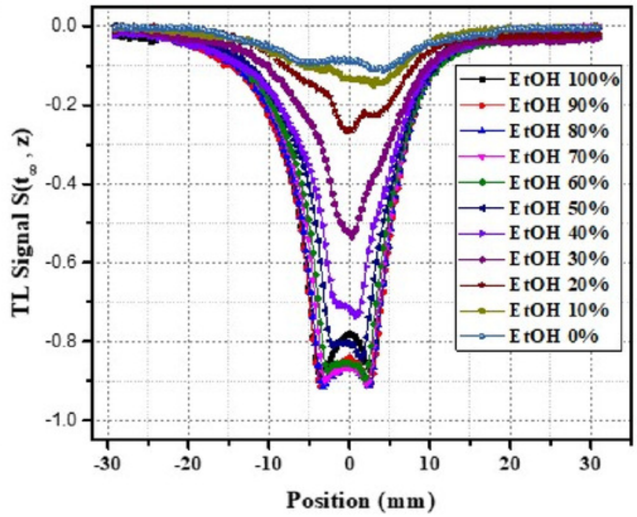
TL Signal S(t∞ , z)
Position (mm)
EtOH 100%
EtOH 90%
EtOH 80%
EtOH 70%
EtOH 60%
EtOH 50%
EtOH 40%
EtOH 30%
EtOH 20%
EtOH 10%
EtOH 0%

(b)

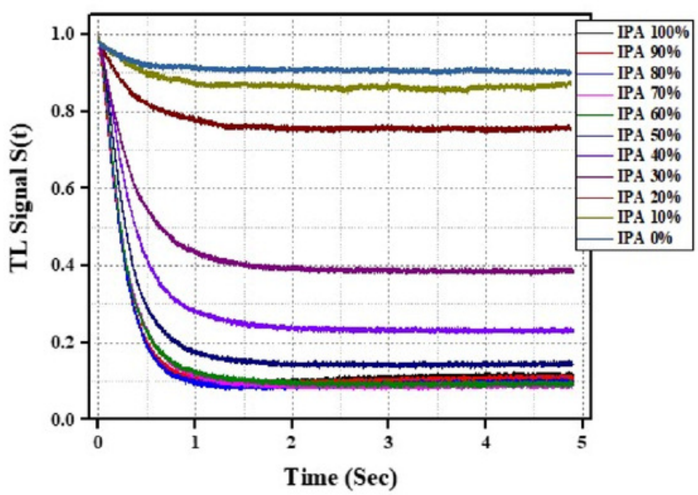
TL Signal S(t)
Time (Sec)
IPA 100%
IPA 90%
IPA 80%
IPA 70%
IPA 60%
IPA 50%
IPA 40%
IPA 30%
IPA 20%
IPA 10%
IPA 0%

(c)

Figure 7

Variation of the steady state TL signal

Variation of the steady state TL signal at various volume fractions of water with (a) different sanitizers, and (b) different solvents.

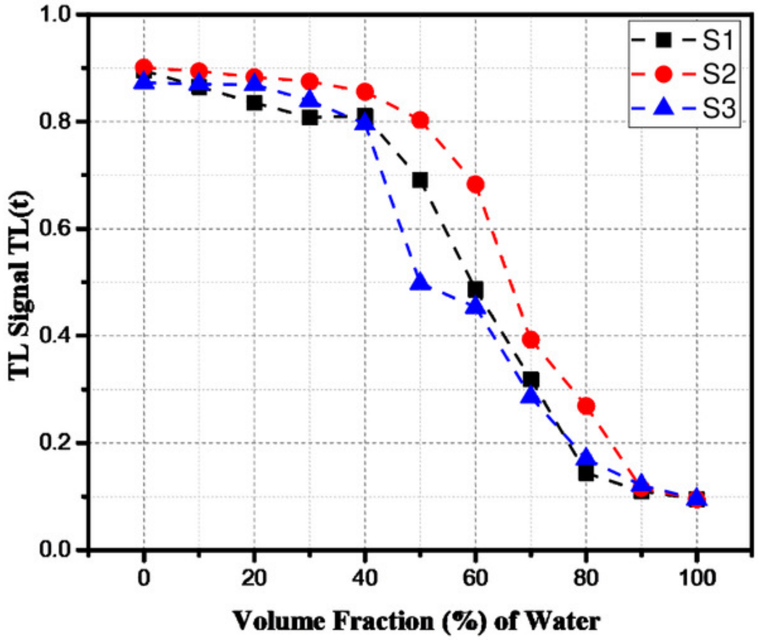
TL Signal TL(t)
Volume Fraction (%) of Water
S1
S2
S3
1.0
0.8
0.6
0.4
0.2
0.0
0
20
40
60
80
100

(a)

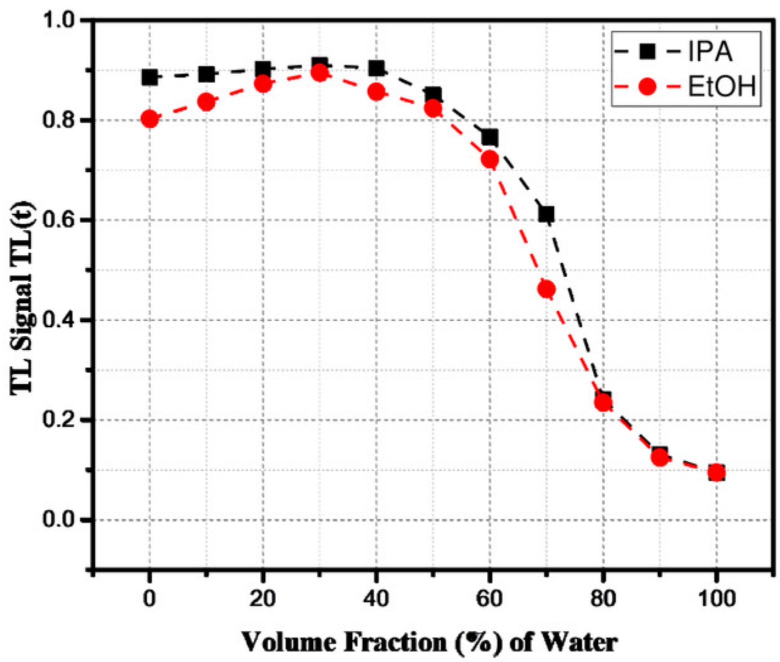
TL Signal TL(t)
Volume Fraction (%) of Water
IPA
EtOH
1.0
0.8
0.6
0.4
0.2
0.0
0
20
40
60
80
100

(b)